Discrimination of tropical forest types, dominant species, and mapping of functional guilds by hyperspectral and simulated multispectral Sentinel-2 data

Postprint version

Gaia Vaglio Laurin, Nicola Puletti, WilliamHawthorne, Veraldo Liesenberg, Piermaria Corona, Dario Papale, Qi Chen, Riccardo Valentini

Published in: **Remote Sensing of Environment**

Reference: Vaglio Laurin, G., Puletti, N., Hawthorne, W., Liesenberg, V., Corona, P., Papale, D., et al. (2016). Discrimination of tropical forest types, dominant species, and mapping of functional guilds by hyperspectral and simulated multispectral Sentinel-2 data. Remote Sensing of Environment, 176, 163-176. doi:10.1016/j.rse.2016.01.017

Web link: http://dx.doi.org/10.1016/j.rse.2016.01.017

This project has received funding from the European Union's Horizon 2020 research and innovation programme under grant agreement No 640176

Remote Sensing of Environment 176 (2016) 163–176

Discrimination of tropical forest types, dominant species, and mapping of functional guilds by hyperspectral and simulated multispectral Sentinel-2 data

Gaia Vaglio Laurin [a,b,*], Nicola Puletti [c], William Hawthorne [d], Veraldo Liesenberg [e], Piermaria Corona [c], Dario Papale [b], Qi Chen [f], Riccardo Valentini [a,b]

[a] Impacts of Agriculture, Forests and Ecosystem Services Division, Euro-Mediterranean Center on Climate Change (IAFES-CMCC), via Pacinotti 5, Viterbo 01100, Italy
[b] Department for Innovation in Biological, Agro-Food and Forest Systems (DIBAF), University of Tuscia, Viterbo 01100, Italy
[c] Consiglio per la ricerca in agricoltura e l'analisi dell'economia agraria, Forestry Research Centre (CRA-SEL), Via Santa Margherita 80, I-52100 Arezzo, Italy
[d] Department of Plant Sciences, University of Oxford, South Parks Road, Oxford OX1 3RB, UK
[e] Santa Catarina State University (UDESC), Av. Luiz de Camoes, 2090, Lages, Santa Catarina 88520-000, Brazil
[f] Department of Geography, University of Hawai'i at Mānoa, 422 Saunders Hall, 2424 Maile Way, Honolulu, HI 96822, USA

abstract

To answer new scientific and ecological questions and monitor multiple forest changes, a fine scale characterization of these ecosystems is needed, and could imply the mapping of specific species, of detailed forest types, and of functional composition. This characterization can be now provided by the novel Earth Observation tools. This study aims to contribute to understanding the innovation in forest and ecological research that can be brought in by advanced remote sensing instruments, and proposes the guild mapping approach as a tool to efficiently monitor the varied tropical forest resources. We evaluated, in tropical Ghanaian forests, the ability of airborne hyperspectral and simulated multispectral Sentinel-2 data, and derived vegetation indices and textures, to: distinguish between two different forest types; to discriminate among selected dominant species; and to separate trees species grouped according to their functional guilds: Pioneer, Non Pioneer Light Demanding, and Shade Bearer. We then produced guild classification maps for each area using hyperspectral data. Our results showed that with both hyperspectral and simulated Sentinel-2 data these discrimination tasks can be successfully accomplished. Results also stressed the importance of texture features, especially if using the lower spectral and spatial Sentinel-2 resolution data, and highlighted the important role of the new Sentinel-2 data for ecological monitoring. Classification results showed a statistically significant improvement in overall accuracy using Support Vector Machine, over Maximum Likelihood approach. We proposed the functional guilds mapping as an innovative approach to: (i) monitor compositional changes, especially with respect to the effects of global climate change on forests, and particularly in the tropical biome where the occurrence of hundreds of species prevents mapping activities at species level; (ii) support large-scale forest inventories. The imminent Sentinel-2 data could serve to open the road for the development of new concepts and methods in forestry and ecological research.

1. Introduction

Tropical forests host the largest biodiversity of terrestrial ecosystems and have a fundamental role in the carbon cycle. Improving the monitoring of tropical forests is an important research issue, relevant to the implementation of climate change related agreements and reporting duties, to biodiversity conservation, and to the definition of sustainable schemes for timber extraction. The understanding of ecological mechanisms can also benefit from improved forest monitoring, as in the case of the dynamics of tree species distribution in different ecosystems, community structures, and spatial distributions of functional traits. For both applied and scientific purposes, the use of Earth Observation (EO) is fundamental, allowing extrapolation of local field information, difficult to collect, to the large extents typical of tropical forests. EO systems that allow for credible measurement, reporting and verification are particularly critical for the successful implementation of REDD+ (Reducing Emissions from Deforestation and Forest Degradation) efforts by the United Nations (UN-REDD, 2013).

The initial remote sensing focus in forest research, a few decades ago, pointed toward the detection of deforestation and forest land conversion, and the coarse characterization of different forest types. These tasks have been successfully accomplished using optical data, which are now a consolidated tool to monitor, at large and medium scales,

* Corresponding author at: Impacts of Agriculture, Forests and Ecosystem Services Division, Euro-Mediterranean Center on Climate Change (IAFES-CMCC), via Pacinotti 5, Viterbo 01100, Italy.
E-mail address: gaia.vagliolaurin@cmcc.it (G. Vaglio Laurin).

different forest features (i.e. extent and changes, productivity, health conditions), thanks to the availability of free, multitemporal, and global satellite datasets (Hansen et al., 2008a; Hansen et al., 2008b; Margono et al., 2012; Zhu, Woodcock, & Olofsson, 2012).

In recent years, a more detailed characterization of forests is needed, to answer new scientific and ecological questions and to monitor change in many attributes, such as the occurrence of specific species, and of detailed forest types and their functional composition. This improved forest characterization can be provided by new EO tools, thanks to the fast technological advancements of this sector.

Satellite open access data presently available (e.g. Landsat, MODIS), however, do not allow for very fine ecological mapping and monitoring, due to limited spatial and spectral resolutions. Despite these limitations, some studies using multispectral satellite data, often in conjunction with microwave data, have been able to derive valuable forest information such as the characterization of forest classes and/or successional stages (Foody, Palubinskas, Lucas, Curran, & Honzak, 1996; Vaglio Laurin et al., 2013); or carbon stock estimation until the saturation limit (Cutler, Boyd, Foody, & Vetrivel, 2012; Foody, Boyd, & Cutler, 2003a; Gibbs, Brown, Niles, & Foley, 2007; Vicharnakorn, Shrestha, Nagai, Salam, & Kiratiprayoon, 2014). Additionally, some hyperspectral systems are available on orbital level such as Hyperion and CHRIS/PROBA: even if spatially limited, they brought new perspectives for tropical rain forest studies (Thenkabail, Enclona, Ashton, et al., 2004, Galvão, Breunig, Santos, & Moura, 2013, Saini et al., 2014; Somers & Asner, 2013).

With airborne sensors, such as LIDAR and hyperspectral, more detailed forest information can be locally derived, with examples including fine scale biomass (Chen, Vaglio Laurin, & Valentini, 2015; Clark, Roberts, Ewel, & Clark, 2011; Dubayah et al., 2010; Pirotti, Vaglio Laurin, Vettore, Masiero, & Valentini, 2014; Vaglio Laurin et al., 2014) and biodiversity estimations (Carlson, Asner, Hughes, Ostertag, & Martin, 2007; Féret & Asner, 2014; Leutner et al., 2012; Vaglio Laurin et al., 2014); forest types (Chan & Paelinckx, 2008) and species composition (Féret & Asner, 2014). However, airborne imagery is characterized by high variability, due to different atmospheric and flight conditions, or sensors used; the generalization of these local findings is rarely possible and the high data acquisition cost prevents the use of airborne tools over large regions or for monitoring purposes. Forest research and monitoring has both the need of open access new high quality satellite data, suitable for repeated monitoring over large areas, and of local data collected with innovative sensors, which are under continuous development and allow for technical and scientific advancements.

Forest types have been defined by the Convention of Biological Diversity as a group of forest ecosystems of generally similar composition that can be differentiated from other such groups by their species composition, productivity and/or crown closure (https://www.cbd.int/forest/definitions.shtml, accessed on June 4th 2015). The identification at fine detail of forest types, successional stages, health conditions and symptoms of vegetation stress, is critical to provide useful information for management and conservation planning (Barbati, Corona, & Marchetti, 2007; Marchetti, Vizzarri, Lasserre, Sallustio, & Tavone, 2014). Vegetation types can be used as a surrogate for modeling the distribution of species and communities (Foody, 2003b); their mapping is important as certain types are more susceptible to change due to climate variability or anthropogenic pressure than others. In the tropical forest region there is a scarcity of fine scale land cover data and forest type maps (Vaglio Laurin et al., 2013), and this information is especially relevant to those areas interested by the REDD + (Reducing Emissions from Deforestation and Forest Degradation) program incentives. Hyperspectral airborne data already proved very useful for detailed forest type characterization. Asner et al. (2011); Kumar, Schmidt, Dury, and Skidmore (2001); Thenkabail, Lyon, and Huete (2011) and Ustin, Roberts, Gamon, Asner, and Green (2004) provided detailed insights on principles and ecological applications of image spectroscopy, which is based on the fine spectral differences captured in hyperspectral data and allow the very fine characterization of forests. Almost two decades ago Martin, Newman, Aber, and Congalton (1998) discriminated among temperate forest types in US using Airborne Visible/Infrared Imaging Spectrometer (AVIRIS) data, and since then many advancements have been made through the detection of vegetation biochemical differences (see Kalacska & Sanchez-Azofeifa, 2008; and Kokaly, Asner, Ollinger, Martin, & Wessman, 2009). Even if image spectroscopy technique is not new, its application in tropical forests for forest type and species mapping is limited by high airborne survey costs, and is more challenging than in other ecosystems due to the high number of spectrally similar species, an irregular phenological behavior, and a complex canopy structure with complicated scattering mechanisms (Baldeck et al., 2014; Clark, Roberts, & Clark, 2005; Papes et al., 2013; Somers & Asner, 2014). Species mapping has proven potential for monitoring invasive or commercially valuable species (Asner et al., 2008; Asner G., R.E, Ford, Metcalfe, & Liddell, 2009; Somers & Asner, 2013). The ESA Sentinel-2 (S2) launch represents a very valuable opportunity for the fine characterization and monitoring of forest types on large scales (Baillarin et al., 2012), and even if this is not an hyperspectral sensor, its innovative features can add value. Sentinel-2 offers a multispectral sensor with 13 bands from 443 to 2190 nm, and a 10 day repeat cycle. The three S2 red edge bands are especially promising for their ability to detect fine differences in chlorophyll pigments; higher chlorophyll content can indicate higher canopy density or complex community structure, or higher nitrogen content in plant tissue (Alvarez-Añorve, Quesada, & De la Barrera, 2008). Despite its potential, the usefulness of S2 for ecological monitoring has been poorly investigated, especially in the tropical biome; examples of research based on simulated S2 data include the monitoring of vegetation status in grassland and savanna in North America (Hill, 2013); the leaf area index estimation in crops in Europe (Richter, Atzberger, Vuolo, Weihs, & d'Urso, 2009), and in four different biomes (Lee, Cohen, Kennedy, et al., 2004); the estimation of leaf chlorophyll content, leaf area index and fractional vegetation cover in a Spanish region (Verrelst et al., 2012). The texture features extracted from S2 bands are also expected to be very useful in forest type classification, as demonstrated by previous studies using textures in tropical forests for this purpose (Li, Lu, Moran, & Hetrick, 2011; Lu, Li, Moran, Dutra, & Batistella, 2014). Texture features, which inform about the spatial relationship between the central pixel of the analysis window and its neighbors, can enhance the features of interest, reducing heterogeneity in the same land cover type and preserving features boundaries. However, the absence of guidelines for the selection of the features of interest, which are dependent on the imagery and bands used, the landscape under investigation, the size of the moving window (Lu, Batistella, Moran, & de Miranda, 2008), limit the extensive application of these useful techniques.

Tree species discrimination is of great interest to support conservation and more sustainable timber extraction practices. Examples of species identification with high resolution hyperspectral data are found in Costa Rica forests, using the HYperspectral Digital Imagery Collection Experiment (HYDICE) sensor (Clark et al., 2005; Clark & Roberts, 2012); in Hawaiian rainforest, where Asner and Vitousek (2005) identified invasive species by quantifying water and leaf nitrogen concentrations with airborne spectroscopy; and again in Hawaiian forest where Féret and Asner (2012) used hyperspectral imagery and LiDAR (Light Detection and Ranging) to map individuals of nine tree species, and Somers and Asner (2012) used time series analysis to detect native and invasive species. To perform species mapping very high spatial resolution sensors are needed, to detect single crowns. In tropical areas the presence of very large crowns helps, but only the very high resolution future hyperspectral satellite missions will support species mapping at reasonable costs over large areas.

Among the different vegetation characteristics studied using remote sensing, one which received much attention is plant functional type, which describes groups of plants with common response to certain environmental influences (Lavorel, McIntyre, Landsberg, & Forbes, 1997;

Lavorel & Garnier, 2002). Functional types are employed in global vegetation and climate change models (Smith, Shugart, & Woodward, 1997; Woodward & Cramer, 1996) because model parameterization is difficult for single species; in this context the Diversitas initiative of the International Geosphere–Biosphere Programme is currently working to refine plant functional classification for the improvement of Earth System models (Canadell, Pataki, & Pitelka, 2007). Evidence of climate change impacts on tropical forests is increasing, and these impacts can produce immediate changes or subtle modifications. Mortality of large trees induced by drought has been documented in Amazon and Borneo forests (Kumagai & Porporato, 2012; Phillips et al., 2010); an increase in above ground biomass and increase in forest dynamics in response to global warming effects have been observed in South American long term monitoring plots (Baker, Swaine, & Burslem, 2003; Lewis et al., 2004). While the effects of extreme events –such as drought and fire induced widespread tree mortality- can be detected by optical data (Zhang et al., 2013), the monitoring of forest modifications induced by long term moderate changes in climate variables, such as a change in functional composition, requires the use of different data and approaches. This is an important research area as the magnitude of functional changes cannot be inferred using structural variables, and climate variability and anthropogenic disturbance are expected to increase in coming years, especially in the West African region (Christensen, Hewitson, Busuioc, et al., 2007; Sheffield & Wood, 2008). Some research has already illustrated climate-related functional changes. For instance, in the Amazon region drought disturbance is a major determinant of forest composition, with differential responses observed in relation to ecological groups and drought types (Karfakis & Andrade, 2013). In Panama, Condit, S.P, and R.B (1996) analyzed forest compositional changes after a sequence of dry years and seasons, finding that a decline in the moisture-demanding guild indicates that a change in composition precedes a structural change. Anthropogenic activities, such as logging, can also modify the guild composition of forests in favor of fast growing pioneer species, as observed in an Indonesian Dipterocarp forest (Yoneda, Nishimura, Fujii, & MUKHTAR, 2009). Assessing forest guilds composition is important also to better understand forest growth dynamics: in Ghana, these dynamics were influenced both by functional composition and resource availability (Baker et al., 2003).

Different kinds of functional groups have been proposed (Reich et al., 2003); Clark and Clark (1999) suggested that in tropical forests the number of groups is potentially very high. One approach of functional grouping relates plant response to illumination condition, such as shade tolerance (Mulkey, Wright, & Smith, 1993). According to this approach Hawthorne (1995) classified West African forest tree species in Pioneer (PION), Non Pioneer Light Demanding (NPLD), and Shade-Bearer (SB) guilds. The guild concept has been used for many years (Simberloff & Dayan, 1991; Terborgh & Robinson, 1986), but many questions related to the structure of ecological communities are still debated, including the processes that promote different dominance of patches of particular guilds. In this respect, the study of disturbances using remote sensing and in situ data is promising (McDowell et al., 2015), as it can clarify the processes that contribute to shape the varied patterns of dominance by different guilds. Studying forests using the guild approach and developing guild mapping initiatives can support community ecology science as well as ecosystem management. The guild approach has already proved effective in tropical areas to assess the effects of disturbance, such as selective logging (Hawthorne, Sheil, Agyeman, Juam, & Marshall, 2012), or forest fragmentation (Hill & Curran, 2005). In Central Amazonia, remote sensing and in situ data were useful to understand the complex large-scale structure of an old-growth forest, which resulted driven by disturbance and recovery cycles (Chambers et al., 2013).

In Ghana, Sheil, Salim, Chave, Vanclay, and Hawthorne (2006) found a trade-off between mature tree size and their shade tolerance or guild, influenced by disturbance, while Fauset, Baker, Lewis, et al. (2012) observed a shift in guilds composition, they proposed, as a response to long term drought. Forest monitoring can also directly benefit from a guild approach, as the proportion of trees belonging to different guilds provides an indication of successional forest conditions. For Ghana this has been illustrated in previous research, through the development of a Pioneer Index (Hawthorne, 1996; Hawthorne & Abu-Juam, 1995). Similarly, guilds have been helpful in other investigations such as the usefulness of different types of secondary vegetation to local communities (Marshall & Hawthorne, 2012); for framing the physiological responses of different tree species to light (Agyeman, Swaine, & Thompson, 1999); for understanding tree allometric relationships (Sheil et al., 2006); and to explore tree species diversity (Bongers, Poorter, Hawthorne, & Sheil, 2009). However, the number of studies addressing guilds composition to monitor and understand forest functional changes is still limited, and additional research and monitoring efforts are needed especially under the present climate change threat.

The present research has three main objectives. The first is to evaluate the ability of airborne hyperspectral data and simulated S2 data, and derived features (vegetation indices and textures) to distinguish between two slightly different forest types in Ghana: wet evergreen forest in Ankasa Conservation Area, and moist semi-deciduous forest in Bia Conservation Area. Our hypothesis is that the two areas are distinguishable with both hyperspectral and S2 data, thanks to the different forest structures and phenological characteristics, even though a significant number of trees of the same species are found in both forests. The second objective is to evaluate the ability of hyperspectral and S2 datasets to distinguish among selected dominant tree species, belonging to different guilds, in each area. We hypothesize that this task can be well accomplished using hyperspectral data and that less accurate results can be obtained using simulated S2 data, due to its more limited spatial and spectral resolutions. The third objective is to test the hyperspectral and S2 datasets for the discrimination of functional guilds, identified as Non Pioneer Light Demanding (NPLD), Pioneer (PION), and Shade-Bearer (SB), according to Hawthorne (1995). We expect that the spectral variation among different guilds is larger than that among species belonging to the same guild, and thus that the trees in our areas can be discriminated, classified and mapped according to the guild they belong to. For classification, performed using hyperspectral data, we adopted and compared Maximum Likelihood and Support Vector Machine approaches. This third objective is closely connected to the aim of improving forest monitoring and assessment. Knowledge of abundance and cover of forest guilds is useful for biodiversity assessment, particularly in tropical forest. Coupling forest inventory and thematic maps, obtained using remote sensing data, can support this effort in two main ways. The first one is the use of thematic maps to improve forest inventory estimates. It is well known that, given a sampling effort (the number of sample survey units), application of stratified sampling techniques to environmental resources leads to more precise population estimates than the non-stratified ones. In the case of stratified sampling, like multi-phase forest inventories, the area is divided into relatively homogeneous subareas (called strata) and each stratum is sampled separately. The single stratum can be obtained directly from thematic maps, like e.g. the guilds map. The second option comes from estimating the relationship between remotely sensed data and forest attribute selected from field inventory, in order (i) to map this forest attribute over the entire region of interest, or (ii) improve the precision of inventory estimates: for methodological details, see Corona (2010).

Overall, these objectives are useful to understand to which extent advanced airborne technology is capable of providing very fine resolution information on forests, for example for tracking subtle forest changes in relationship to climate variability, and which part of this information is lost or preserved when using spatially and spectrally coarser data such as the new satellite S2, which on the other hand allows for broader area coverage and absence of data acquisition costs.

2. Materials and methods

2.1. Study areas

The Ankasa Conservation Area (Fig. 1) is located in south-western of Ghana, covering an area of 509 km^2; it is composed by the Nini-Suhien National Park and the Ankasa Resource Reserve. It became a wildlife protected area in 1976. The climate is characterized by a bi-modal rainfall pattern, from April to July and from September to November; an average annual rainfall between 2000 and 2200 mm; a mean monthly temperature typical of tropical lowland forest and ranging from 24 °C to 28 °C; and a relative high humidity throughout the year, from about 90% at night to 75% in early afternoon. The vegetation of Ankasa is characterized as wet evergreen forest, with high floristic and structural diversity and restricted to the highest rainfall zone in Ghana (Hall & Swaine, 1981). Species typical of this forest zone include: Cynometra ananta, Lophira alata, Heritiera utilis, and Protomegabaria stapfiana. Two species that are very common in the semi-deciduous forests of central Ghana, Celtis mildbraedii and Triplochiton scleroxylon, are absent from Ankasa. The landscape is characterized by the presence of low hills with an average elevation of 90 m a.s.l. and swampy areas. The geological substrate of the reserve is mainly granite of the Cape Coast complex. Parts of the southern portions of this forest were selectively logged from about the 1960s to 1974, but logging intensity was low due a small proportion of valuable timber species, and most of the forest was untouched (Hawthorne, 1989).

The Bia Conservation Area (Fig. 1) is located in the Juabeso-Bia District in southwest Ghana close to the border with Ivory Coast, covering approximately 306 km^2. It comprises the Bia National Park (northern part) and Bia Resource Reserve (southern part) and covers the transition zone between two of Ghana's forest types, moist evergreen forest in the south and moist semi-deciduous forests in the north. It is characterized by a bimodal rainfall peaks, between May and June and between September and October; a mean annual precipitation ranges from 1500 to 1800 mm; and a mean monthly temperature ranges between 24 °C and 28 °C (Hall & Swaine, 1981). Some of the most common species are: Baphia nitida, Celtis mildbraedii, Pycnanthus angolensis, Triplochiton scleroxylon, and Terminalia superba (Hawthorne, 1995). The topography of the study area is generally hilly with elevations ranging between 168 m and 238 m a.s.l. The geological formation corresponds to the Lower Birrimian. In Bia National park no systematic logging activity occurred in the past decades, while selective logging was relatively intense in southern Bia Resource Reserve until the beginning of the nineties (Hawthorne et al., 2012).

2.2. Remote sensing data and photointerpretation

Airborne hyperspectral data were collected in two consecutive days on March 2012, in strips covering parts of the study areas, with an AISA Eagle sensor with FOV equal to 39.7 urad, a signal-to-noise ratio of 1250:1, set to record 244 bands with 2.3 nm spectral resolution in the 400–1000 nm range, and resulting in a spatial resolution of 1 m after radiometric correction and orthorectification (Fig. 2). The Fast Line-of-Sight Atmospheric Analysis of Spectral Hypercubes (FLAASH) algorithm (Felde et al., 2003) was used to perform the atmospheric correction of the strips. Fifty-two noisy bands out of the 450–900 nm range and four bands between 759 and 766 nm range were removed, obtaining 186 bands. We used Minimum Noise Fraction (Green, Berman, Switzer, & Craig, 1988) to remove or reduce the noise in the spectral curve of each pixel; for each strip we retained only the MNF components (9 to 15) in which the crown shapes were still visible and not confused by noise, excluding the other noisy ones; we finally converted the MNF bands to the original scale so that we can calculate the spectral indices, as in other studies (Galvão, Formaggio, & Tisot, 2005; Shafri, Hamdan, & Izzuddin Anuar, 2012). For the present analysis we performed a systematic sampling, selecting one band every 15 to obtain 13 bands, to ensure that the bands were evenly distributed across the 450 to 900 nm spectral range. Furthermore, using bands from the full dataset we computed the following vegetation indices: Normalized Difference Vegetation (NDVI) and Simple Ratio (SRI) (Sellers, 1985), Atmospherically Resistant Vegetation (ARVI) (Kaufman & Tanré, 1996), Red Edge Normalized Difference Vegetation (ReNDVI) (Sims & Gamon,

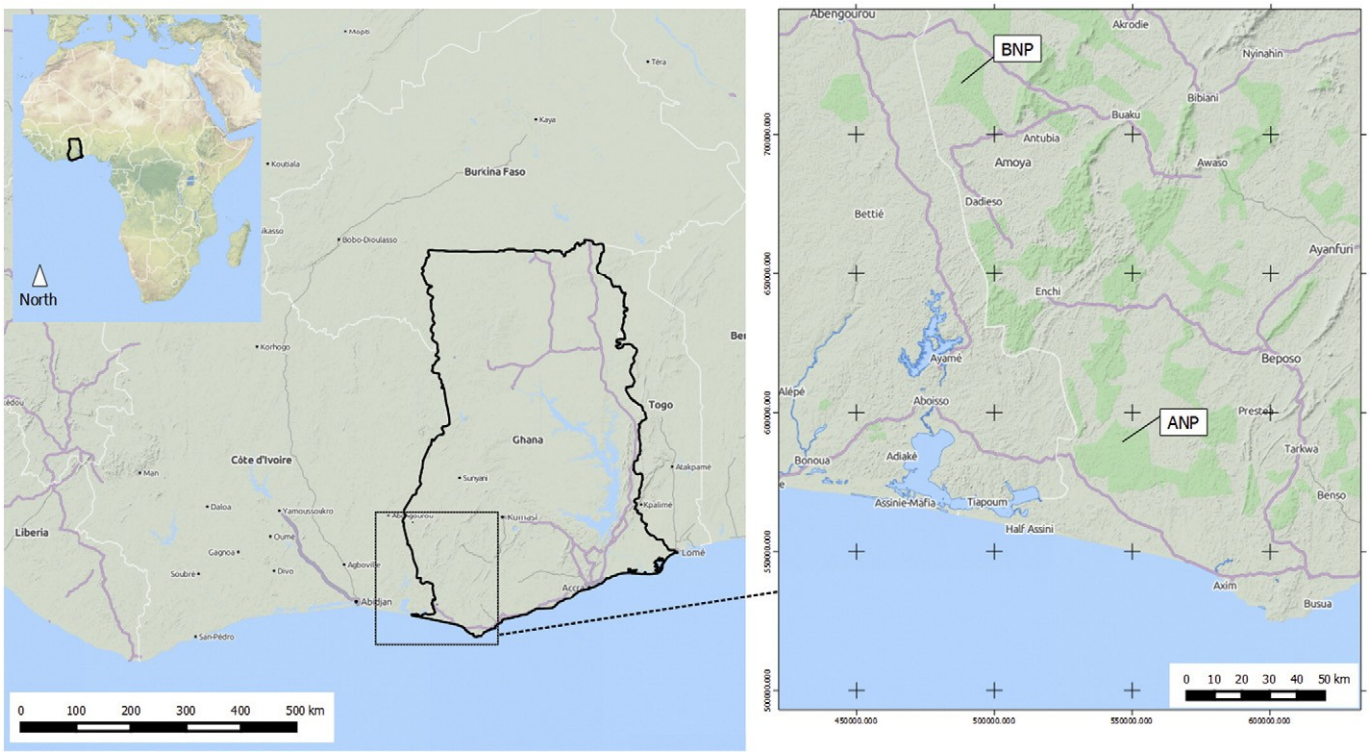

Fig. 1. Location of Ankasa (ANP) and Bia (BNP) Conservation Areas.

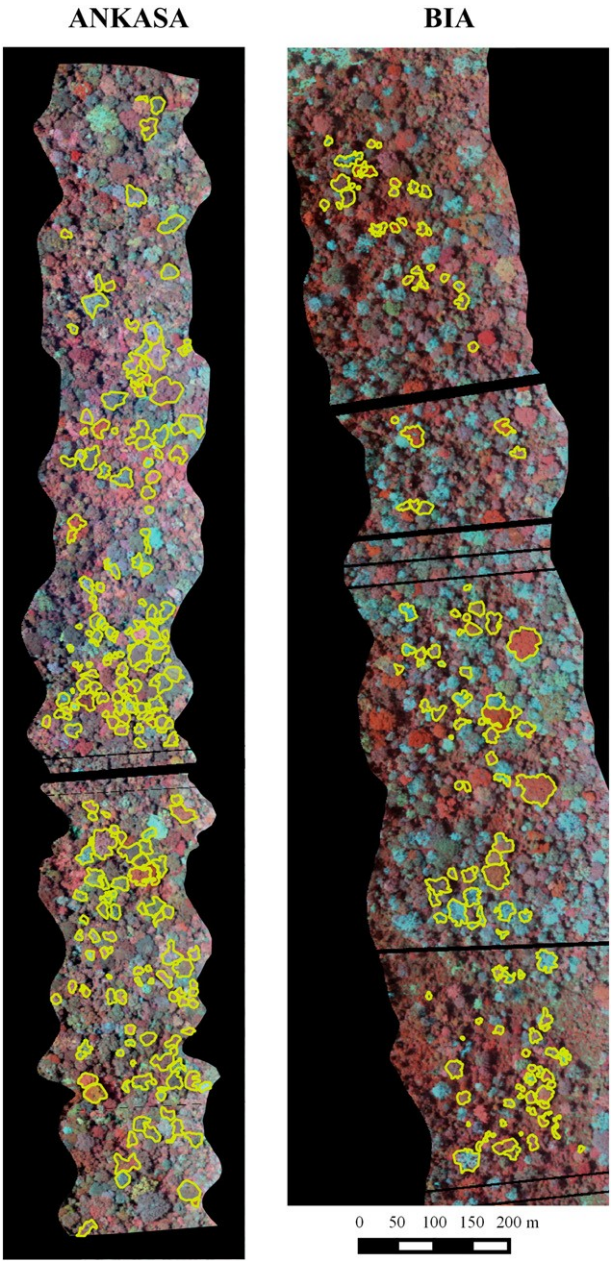

Fig. 2. Hyperspectral data collected over Ankasa and Bia Conservation Areas in a false color composite of 829 nm (R), 604 (G), and 465 (B) bands. The yellow polygons represent the delineated crown species.

2002), Vogelmann Red Edge (VReI) (Vogelmann, Rock, & Moss, 1993), Photochemical Reflectance (PRI) (Gamon, Penuelas, & Field, 1992), Red Green Ratio (GRI) (Gamon & Surfus, 1999), Carotenoid Reflectance1 and 2 (CRI1, CRI2) (Gitelson, Zur, Chivkunova, & Merzlyak, 2002), and Anthocyanin Reflectance 1 and 2 (ARI1, ARI2) (Gitelson, Merzlyak, & Chivkunova, 2001). MNF and vegetation indices were computed using the ENVI software (Excelis); criteria for band assignment are described in http://www.exelisvis.com/docs/spectralindices.html (accessed on 22nd October 2015). We also computed Gray Levels Co-Occurrence Matrix (GLCM) Mean, Variance, Homogeneity, Contrast, Dissimilarity, Entropy, Second Moment and Correlation textural features (Haralick, 1979) using a 5 × 5 window size, consistent with crowns dimension in our sites (generally comprised between 5 and 15 m radius).

Aerial photographs, used to identify and delineate tree crowns, were acquired simultaneously with hyperspectral data with a Rollei H25 camera equipped with a Phase One Digital Back. Images were georeferenced and orthorectified using a lidar DEM available for the study areas (Vaglio Laurin et al., 2014) in ENVI software (Excelis); orthophotos were acquired at 0.1 m spatial resolution.

Using hyperspectral imagery we simulated most of the data which will be collected by the multispectral sensor mounted on the ESA S2 satellite mission, launched on 23rd June 2015 (Fig. 3). Due to the limited spectral range of our hyperspectral data (450–900 nm), bands 1 and 9 were not simulated, as well as all the bands (10, 11, 12) included in the short wave infrared portion of the spectrum. The remaining 8 bands were simulated using the Spectral Response Functions (SRF) and the approach developed by D'Odorico, Gonsamo, Damm, and Schaepman (2013). Bands were centered at 490, 560, 665, 705, 740, 783, 842 and 865 nm. All bands' spatial resolution was set to 10 m, resampling with nearest neighbor algorithm the four bands (705, 740, 783 and 865 nm) simulated at 20 m according to SRF; in fact, for test purposes we chose to set the spatial resolution equal for all the bands, even those which are planned at 20 m in the actual S2 sensor. According

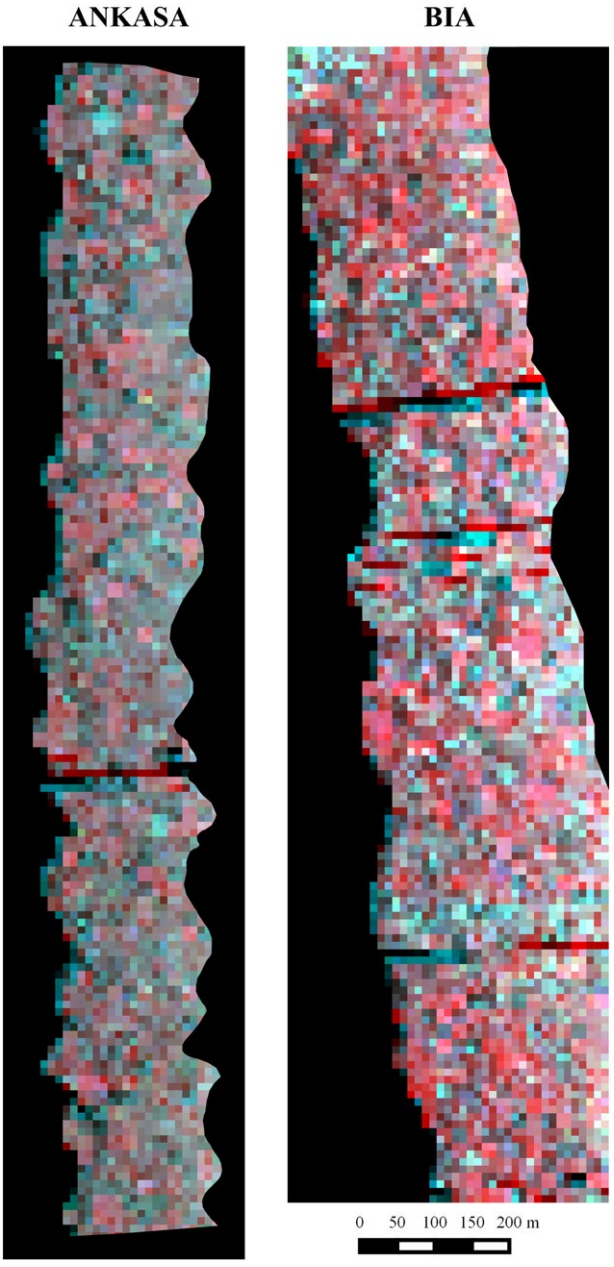

Fig. 3. Simulated Sentinel-2 data derived from hyperspectral strips collected in Ankasa and Bia Conservation areas. False color composite of bands 8 (R), 3 (G), 2 (B).

the available bands, we were able to calculate four vegetation indices (NDVI, SRI, RENDVI, ARI1) and the Gray Levels Co-Occurrence Matrix (GLCM) textural features (Haralick, 1979) using the smallest possible (3 × 3) window size.

Using 10 cm resolution orthophotos we delineated the crowns of species for which identification was unequivocal for their phenological characteristics in the surveyed period, and which were covered by quality data (haze and cloud free). This species identification (including 6 species listed in Table 1, and other 15 representing the different guilds) was possible thanks to the 10 cm resolution of the orthophotos, which allowed the identification of species-specific traits related to crowns structure, foliar texture and color, and in some cases, flowers; when the species identification was uncertain, that species was discarded from the analysis. Identification was guided by ground truth, plot data. Results where then reported to the 1 m resolution co-registered hyperspectral images (Fig. 2), overlaying the interpreted tree species with hyperspectral images, and consequently to the simulated S2 dataset. To refine the results of the photointerpretation, we used field data provided by the ERC Africa GHG FP7 EU funded project, which collected data in different surveys carried out in 2012–2013. Overall, during the surveys, 4.7 ha (899 trees) were surveyed in Ankasa and 3.89 ha (575 trees) in Bia, collecting information on species, height and diameter at breast height (DBH) for trees ≥20 cm DBH. We also collected field information on lianas presence: this helped during the photointerpretation to exclude crowns on which lianas were densely superimposed, which however were few, spread between the more globular and discrete tree crowns, and characterized by a different texture due to their different architecture. We did not have accurate geographical coordinates for single trees, but we checked if the species with larger crowns identified in the orthophotos were also recorded (with large DBHs) in the field records. The use of photointerpretation with ground truth data was the only possible solution in complex ecosystems like the one under analysis, where the number of species and complexity of vertical canopy structure make a correct and spatially extensive mapping of the crowns unfeasible.

2.3. ROI delineation

Two Region of Interest (ROI) of about 26 ha were selected on hyperspectral imagery inside the reserves, avoiding boundary zones (exactly of 258,346 1 × 1 m pixels for Ankasa and 259,353 for Bia). In simulated S2 dataset these two regions corresponded to 2588 and 2593 pixels, respectively. These 'area ROIs' were used to test the separability of the two wet evergreen and moist semi-deciduous forest types.

ROIs of crowns of three dominant species per site were identified, with dominance due to high number of individuals in the upper canopy layer determined by visual inspection of high resolution imagery (Table 1); crowns were further screened to retain only the larger ones, evenly distributed spatially, with species equally represented, thus obtaining a similar number of pixels for each species. These 'species ROIs' were used to test the separability among canopy dominant species inside the Ankasa and Bia sites.

ROIs of crowns for 15 species, almost equally represented and belonging to PION, SB, and NPLD guilds, were also delineated to obtain in each area a similar number of pixels per guild type (Table 3). The PION species included: Alstonia boonei, Elaeis guineensis, Lophira alata, Myrianthus arboreus, Terminalia superba, Triplochiton scleroxylon; the SB: Berlinia spp., Celtis mildbraedii, Cola gigantea, Cynometra ananta; and the NPLD: Albizia spp., Heritiera utilis, Piptadeniastrum africanum, Protomegabaria stapfiana, Pycnanthus angolensis, and Uapaca guineensis. These 'guilds ROIs' were used as a preliminary test for the separability at guild level per area, and then to produce the guilds maps by means of the two different classification approaches. Ghana has more than 300 large forest tree species (Hawthorne & Gyakari, 2006), so this is a first examination of this approach. For classification purposes, a 'Shadow' class of similar size was also delineated in each area. All the classes (NPLD, PION, and SB) were randomly partitioned into 70% training and 30% validation sets.

2.4. Classification procedure

We adopted and compared the results of two classifications. Maximum Likelihood (ML) approach (Richards & Jia, 1999) was selected due to its broad diffusion. Support vector machine (SVM) is a supervised non-parametric statistical learning technique, which is known for the ability to generalize well even with limited ground truth, and often used to improve the classification of remotely sensed imagery, including airborne hyperspectral (Féret & Asner, 2012; Mountrakis, Im, & Ogole, 2011; Paneque-Gálvez et al., 2013). With ML technique, training multidimensional data are used to find the so-called optimal separation hyperplane, i.e. the hyperplane that separates the dataset into a discrete predefined number of classes in a way consistent with training sample, maximizing the distances between different classes in order to minimize misclassifications (Burges, 1998). To perform ML we used ENVI 4.5 (Exelis). For SVM we adopted the R package e1071 (R Core Team, 2013); the optimal gamma and cost parameters were identified using tune.svm function. For both Ankasa and Bia gamma was equal to 0.1 and cost equal to 10. ML and SVM results for each area were compared using the Z test (Congalton & Green, 2008); test values ≥1.96 (at 95% confidence level) indicate that the confusion matrices under comparison are significantly different.

2.5. Data analysis steps

The first step was to analyze the separability of Ankasa and Bia forests. We used the Jeffrei–Matusita (J-M) separability measurement (Richards & Jia, 1999) and the 'area ROIs' to test the ability of hyperspectral, simulated S2 data, and the vegetation indices derived from these datasets, to distinguish the two different forest types. The value of the J-M measurement ranges from 0 to 2.0 and indicates how well the selected ROI pairs are statistically separated; values above 1.8 indicate that the ROI pairs have good separability (Richards & Jia, 1999).

As second step, we repeated the separability analysis at crown level for the 3 dominant species in each area, using 'species ROIs', represented by a relevant number of pixels (≥40 in simulated S2 data) and belonging to different guilds, using as input the same hyperspectral, simulated S2, and derived features. This test highlighted the separability of different species (and their guilds) inside each area.

We finally used the 'guild ROIs' to investigate the separability of different guilds over the entire airstrips, by means of hyperspectral, simulated S2 and derived features.

Table 1
Selected dominant species for Ankasa and Bia areas, pixels in hyperspectral and simulated Sentinel-2 data, and guild type. S2 = simulated Sentinel-2. NPLD = Non Pioneer Light Demanding; PION = Pioneer; SB = Shade-Bearer.

Ankasa conservation area				Bia conservation area			
Species name	Hyper pixels	S2 pixels	Guild	Species name	Hyper pixels	S2 pixels	Guild
Cynometra ananta	4607	57	SB	Pycnanthus angolensis	4670	55	NPLD
Heritiera utilis	4373	59	NPLD	Terminalia superba	4578	52	PION
Protomegabaria stapfiana	4452	45	NPLD	Triplochiton scleroxylon	4739	56	PION

When the separability threshold (set to 1.8) was not reached with bands or vegetation indices as inputs, we added texture features as inputs. To avoid using a very large number of textures we adopted a simple and semi-automatic approach for selecting the most relevant ones for each separability task (forest type, species, and guilds distinction). We first stacked (joined the features in a stack, ie. a single file for processing purposes) all the textures of a given type (e.g. mean, variance etc.) and ranked their J-M scores (by type stacking); layer stacking and J-M analysis were performed with ENVI (Excelis) software. We then stacked the textures according to the band they derived from, and again ranked the J-M scores obtained (by band stacking). We then added to the original bands or vegetation indices (if the latter performed better than bands) a number of progressively higher texture features, until the 1.8 set threshold was reached. The added textures were those having the higher rank in by type stacking, generated from bands (maximum four) that obtained better scores in by band stacking. Finally, we produced tree guilds maps, one per area, from the hyperspectral imagery.

3. Results

3.1. Differentiation of forest types based on spectral properties, vegetation indices, and texture

We tested the J-M separability of the two Ankasa and Bia areas using the 13 systematically sampled hyperspectral bands and derived vegetation indices. J-M with 13 bands as inputs resulted N1.99, and the same result was obtained using all the computed vegetation indices. To identify the most informative spectral regions we tested J-M measurement separately per each index; most of them obtained scores well above the 1.8 separability threshold, with the exception of three indices with scores between 0.63 and 1.52 (ARI1, CRI1, and SRI). We repeated the separability using only the highest scoring vegetation indices, REPI and SGI indices, obtaining a J-M score N 1.99. Overall, these results indicate that the two areas can be easily discriminated using both original hyperspectral data and the derived indices. The most informative spectral regions were the red edge and the green.

The J-M scores for the eight S2 simulated bands were equal to 0.70; the score increased to 0.98 when the four vegetation indices were used as input. To increase separability we added texture features. The semi-automatic procedure of texture selection resulted in the selection of variance, contrast, and dissimilarity from bands 1, 2, and 3. The J-M score obtained using these textures and the 4 vegetation indices as inputs was equal to 1.89. These results indicate that the two areas can be distinguished by simulated S2 data, using derived features (vegetation indices and textures), while the task cannot be accomplished using the S2 bands or vegetation indices alone.

3.2. Differentiation of dominant species based on spectral properties, vegetation indices, and texture

The results presented in this section are related to the differentiation of dominant species. Three species were considered in each area: Table 1 illustrates the results obtained from the delineation of crowns, with number of crowns for each species comprised between 12 and 38; the separability of the dominant species in Ankasa and Bia areas according to different inputs is reported in Table 2.

Hyperspectral sampled bands and derived vegetation indices were not able to perform the species distinction in Ankasa. The texture selection procedure previously described resulted in the addition, to the 13 hyperspectral bands, of mean, variance, second moment and correlation textures derived from bands 1 (465.05 nm), 5 (504.42 nm), and 6 (639.99 nm). Results, illustrated in Table 2, indicate that in Ankasa the discrimination between species is only possible with the addition of texture variables. Texture features were particularly useful in the species level analysis, as some of them were able to enhance crowns edges in the imagery (Fig. 4).In Bia, hyperspectral bands or indices were only able to distinguish the two NPLD species pair, but vegetation indices produced J-M scores close to separability threshold for all three pairs of species compared. The procedure of selection of texture features resulted in the addition, to vegetation indices, of mean texture from bands 1 (465.05 nm), 8 (711.17 nm), and 9 (746.93 nm). In contrast to what was found for Ankasa, with the addition of texture, all three pairs had J-M indices N1.8, indicating good separability, and in general, the Bia pairs were more distinguishable than the Ankasa ones.

For simulated S2 data (Table 2), neither the bands nor the vegetation indices were effective in discriminating species in any of the areas. In Ankasa separability was reached when using in addition to bands, second moment, variance, and correlation from bands 1, 2, and 5, according to the results of the texture features selection procedure. In Bia the texture selection resulted in the selection of correlation calculated from bands 2, 3, and 4; with these inputs separability was reached.

Even if simulated S2 results should be interpreted with caution for the limited number of pixels used in the analysis (Table 3), they support what was found with hyperspectral data, namely that the pairs distinction in Bia was easier in comparison to the one in Ankasa, and that the pair composed by two NPLD species showed different behaviors in each area.

3.3. Guilds differentiation and classification results

The results presented in this section are related to the differentiation of guilds, and the following classification exercise. Table 3 provides information on the number of pixels belonging to each guild, in each area, for hyperspectral and simulated S2 data, while the separability of guild in each area according to different inputs is reported in Table 4.

Table 2
J-M scores for pairs of selected dominant species per area, belonging to various guilds (species here are indicated only by genus name, for complete name refer to Table 1). S2 = simulated Sentinel-2. NPLD = Non Pioneer Light Demanding; PION = Pioneer; SB = Shade-Bearer.

Ankasa conservation area						
	Hyper bands	Hyper vegetation indices	Hyper bands + textures	S2 bands	S2 vegetation indices	S2 bands + textures
Cynometra (SB)-Heritiera (NPLD)	1.49	1.46	1.97	1.02	0.83	1.80
Cynometra (SB)-Protomegabaria (NPLD)	1.37	1.45	1.81	1.01	0.36	1.97
Heritiera (NPLD)-Protomegabaria (NPLD)	1.29	1.14	1.80	0.99	0.72	1.98

Bia conservation area						
	Hyper bands	Hyper vegetation indices	Hyper bands + textures	Sentinel-2 bands	Sentinel-2 vegetation indices	Sentinel-2 bands + textures
Pycnanthus (PION)-Terminalia (NPLD)	1.67	1.75	1.84	1.22	0.57	1.93
Pycnanthus (PION)-Triplochiton (NPLD)	1.61	1.79	1.87	1.29	0.57	1.91
Terminalia (NPLD)-Triplochiton (NPLD)	1.90	1.98	1.99	1.55	1.29	1.95

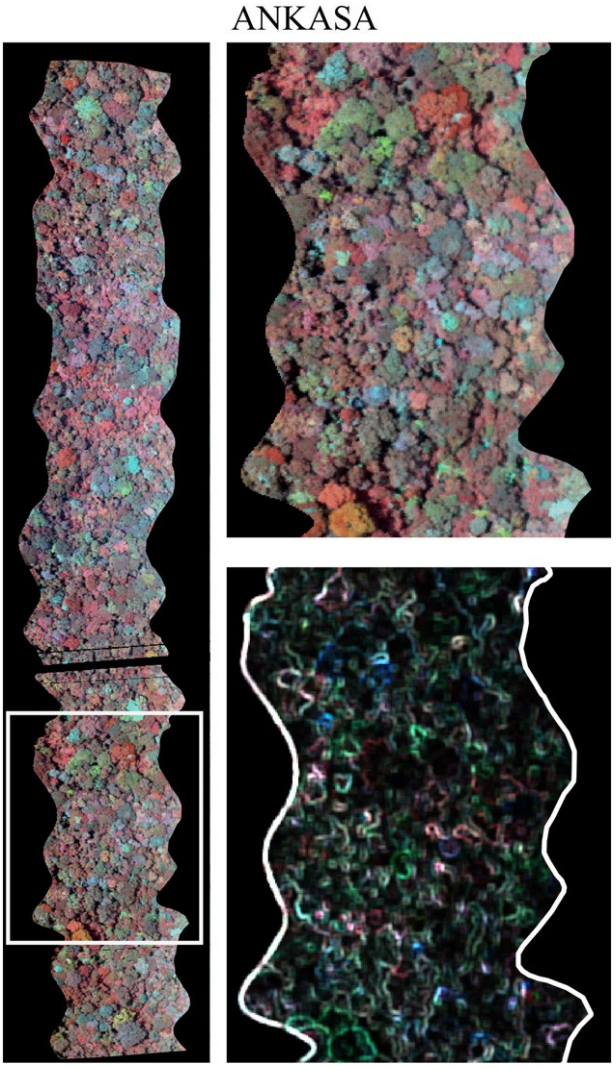

Fig. 4. Ankasa hyperspectral data. On the left hand the hyperspectral strip over Ankasa Conservation Area: false color composite of 829 nm (R), 604 (G), and 465 (B) bands. On the upper right hand a zoom of the left image for the white. Delineated region; on the lower right hand the same regions is shown using a false color composite of variance textures from bands 1 (R), 5 (G), and 6 (B) which highlight crowns edges.

In Ankasa, the hyperspectral sampled bands were not able to separate guild pairs; vegetation indices were successful for both SB-PION and PION-NPLD pairs, with SB-NPLD resulting very close to the 1.8 selected threshold. To reach full guilds discrimination the combination of spectral bands with a subset of the vegetation indices (SGI, PRI, EVI, NDVI, RGRI) was needed. In Bia, nor hyperspectral bands neither indices were successful while, as in Ankasa, the combination of the two sets was able to separate all the guilds pairs. In both areas, the pair most difficult to be distinguished is the SB-NPLD one, and SB-PION is the easiest one. This is consistent with the amount of spectral difference among guilds,

Table 3
Number of pixels from several trees species belonging to different guilds per area. S2 = simulated Sentinel-2. NPLD = Non Pioneer Light Demanding; PION = Pioneer; SB = Shade-Bearer.

Ankasa conservation area				Bia conservation area			
Guild	# of species	Hyperpixels	S2 pixels	Guild	# of species	Hyperpixels	S2 pixels
NPLD	6	2576	30	NPLD	3	2354	26
PION	2	2487	31	PION	4	2369	28
SB	5	2632	29	SB	3	2346	27

which is expected to be larger between SB and PION, with NPLD being intermediate between SB and PION. The larger SB-PION difference is in accordance with the different leaves pigments and structure associated to the two opposite illumination conditions (shade and sunlight exposure).

For simulated S2 data, the bands and the vegetation indices showed low separability values in both areas. For S2, we did not tested the combination of bands and indices as the latter are computed using the eight simulated bands (while for hyperspectral data the indices are computed using other bands than those thirteen sampled). Therefore we added textural features to the S2 bands: for Ankasa the selected ones were correlation from bands 1, 4, and 6; for Bia correlation from bands 1, 2, and 5. The number of pixels used in these tests was low (Table 1), but most of the results confirmed what was found using hyperspectral data with respect to easiness of the separability task for the different type of guilds.

3.4. Guild maps

We produced guilds maps for the entire hyperspectral airborne strips of Ankasa and Bia areas, using as inputs the combination that provided better separability (bands and vegetation indices), and as training and validation the 'guilds ROIs'. Overall accuracy values and K coefficients for the confusion matrices obtained from ML classification are presented in Table 5. Results from SVM are presented in Table 6, and the corresponding maps in Fig. 5. The Z test values were significant for both Ankasa (2.28) and Bia (4.66) areas, indicating that SVM statistically significantly improved the classification results compared to the ones from ML.

We did not attempt the production of guild maps with simulated Sentinel-2 data due to the limited number of available pixels, but the separability analysis in Table 4 indicate that guild maps could be possibly obtained also with these data, especially if exploiting the additional bands, here not simulated, which are planned for the S2 sensor.

4. Discussion

4.1. Forest types

Our first hypothesis, regarding the capability of hyperspectral and S2 data types to distinguish Ankasa and Bia forest types, is supported by the results of J-M measurements obtained in tests using hyperspectral bands or simulated S2 vegetation indices with textures. These forest types discrimination results confirm the known ability of airborne hyperspectral data to perform detailed forest type mapping, and are in line with other research in the tropical biome which evidenced the advantages of using hyperspectral data: for instance, Thenkabail et al. (2004) used Hyperion imagery to classify nine rainforest types in Africa; Held, Ticehurst, Lymburner, and Williams (2003) used both hyperspectral and radar remote sensing to map at high resolution tropical mangrove ecosystems; Kalacska, Bohlman, Sanchez-Azofeifa, Castro-Esau, and Caelli (2007a); Kalacska, Sanchez-Azofeifa, Rivard, et al. (2007b) used image spectroscopy to estimate the diversity of dry forests in Costa Rica. Forest type discrimination using S2 simulated data was less clear, due to the lower spatial and spectral resolution. The positive S2 result stresses the impact that the forthcoming mission could have in ecological mapping and monitoring. We had to add texture information to simulated bands in order to obtain separability.

For S2, it is expected that the availability of additional bands, especially those in the short wave infrared region carrying carbon (lignin, cellulose), nitrogen, and water content information, together with the planned multitemporal acquisitions and thus the ability to capture phenological differences along time, will further improve the ecological monitoring power of the S2 sensor, opening new roads in forest and ecology research.

Using high spectral and spatial resolution inputs, we found that vegetation indices from the red edge and green regions resulted in

Table 4
J-M scores for pairs of guilds per area. S2 = simulated Sentinel-2. NPLD = Non Pioneer Light Demanding; PION = Pioneer; SB = Shade-Bearer.

Ankasa conservation area						
	Hyper bands	Hyper vegetation indices	Hyper bands + veget. Indices	S2 bands	S2 vegetation indices	S2 bands + textures
SB–NPLD	1.53	1.77	1.82	1.23	0.77	1.96
PION–NPLD	1.78	1.90	1.92	1.41	0.45	1.97
SB–PION	1.76	1.86	1.91	1.62	1.11	1.97

Bia conservation area						
	Hyper bands	Hyper vegetation indices	Hyper bands + veget. indices	Sentinel-2 bands	Sentinel-2 vegetation indices	Sentinel-2 bands + textures
SB–NPLD	1.31	1.53	1.83	1.21	1.87	1.80
PION–NPLD	1.74	1.90	1.99	1.47	1.94	1.97
SB–PION	1.71	1.86	1.98	1.54	1.17	1.97

better J-M scores, being highly informative: they alone provided forest type separability. The vegetation indices were calculated from the original 186 bands, so their information content was not necessarily a replication of what was included in the 13 regularly sampled bands. The green spectral portion is partly linked to photosynthetic pigments, but also to non-photosynthetic anthocyanins, which absorb light in this region and are associated with the resistance of plants to environmental stresses such as drought, low nutrients, and high radiation (Viña & Gitelson, 2011). In our study, the red edge and green indices were able to capture the specific differences in canopy density and resistance to drought: these differences are occurring between wet evergreen and moist semideciduous forest types, with the latter type in Bia being characterized by less complex and more open forest structure and species adapted to cope with water scarcity, compared to those in Ankasa.

At the lower resolutions of the simulated S2 bands, texture information was necessary for the discrimination of Ankasa and Bia forests, as well as for the dominant species and guilds distinction tasks. With our semi-automatic empirical method we were able to identify the most useful features, which resulted to be different according to the sites and the different levels of analysis (area, species, and guilds levels). However, in our S2 tests the correlation, which is a statistical measure of the linear dependency of gray levels on those of neighboring pixels, was the most frequently selected feature (four cases out of five) and alone provided separability in three cases; while with respect to bands, band 1 and 2 were the most frequently selected, again in four cases out of five. The texture usefulness is in agreement with several studies conducted in tropical forests that already stressed the importance of texture for land cover classification (Li et al., 2011; Lu et al., 2014; Rakwatin et al., 2012; Vaglio Laurin et al., 2013), or for estimating forest attributes such as biomass and biodiversity (Culbert et al., 2012; Cutler et al., 2012).

4.2. Dominant tree species

The discrimination of the selected dominant tree species in Ankasa and Bia forests required the use of textures with both data types (Table 3). Hyperspectral data are known to allow the discrimination of selected tropical species, thus the results we obtained using this dataset confirm our hypothesis, and are in agreement with previous research based on the full 400–2500 hyperspectral range (Asner & Vitousek, 2005; Clark et al., 2005; Clark & Roberts, 2012; Féret & Asner, 2012). We based our tests on the limited visible to near infrared range, which in certain cases is successful too, such as in the study conducted in Malaysia by Hasmadi, Kamaruzaman, and Hidayah (2010), that performed tree species mapping with hyperspectral data in a range (500–850 nm) similar to the one we employed.

Refuting our second hypothesis, the species discrimination succeeded not only with hyperspectral but also with simulated S2 data. The large crowns (most N10 m radius) characterizing our sites can have a role in this positive result, reducing the impact of the lower spatial resolution of this dataset.

We recognize that in tropical forests, especially the more disturbed ones, lianas, epiphytes and other non-structural elements have the potential to confuse the hyperspectral tree signature, as previous research shown (Castro-Esau, Sánchez-Azofeifa, & Caelli, 2004; Kalacska et al., 2007b; Sánchez-Azofeifa & Castro-Esau, 2006; Zhang, Rivard, Sánchez-Azofeifa, & Castro-Esau, 2006). Additional remote sensing research is needed to properly address this topic and to better understand the impacts of non-structural forest community elements on research and monitoring results.

For our preliminary assessment of guild separability using hyperspectral inputs (Table 2) we emphasize that a few token examples from the hundreds of species in each guild have been taken, and these results cannot be seen as representing the full range of species in each guild accurately. In Ankasa the threshold was barely reached for the two species belonging to the same guild (NPLD), while species from different guilds obtained much better J-M scores. In Bia it was more difficult to separate the two NPLD − PION pairs, compared to the species from the same guild (NPLD); this was also observed using simulated S2 inputs. We expected to find more differences in the foliar biochemical composition of species from different guilds than from the same guild, as the photochemical and pigments composition is largely determined by the solar radiation to which the leaves are exposed. However, during the airborne survey period (dry season) certain species - even if

Table 5
Percentages of user and producer accuracies, overall accuracy and K coefficient for Ankasa and Bia guild maps, using Maximum Likelihood classification algorithm. NPLD = Non Pioneer Light Demanding; PION = Pioneer; SB = Shade-Bearer.

	Ankasa conservation area		Bia conservation area	
	Producer accuracy %	User accuracy %	Producer accuracy %	User accuracy %
SB	84.88	88.10	71.76	88.78
NPLD	88.86	87.71	88.75	60.43
PION	93.88	88.47	87.41	88.89
SHADOW	95.61	98.37	93.12	99.28
Overall accuracy	90.73		84.30	
K coefficient	0.97		0.84	

Table 6
Percentages of users and producers accuracies, overall accuracy and K coefficient for Ankasa and Bia guild maps, using SVM classification algorithm. NPLD = Non Pioneer Light Demanding; PION = Pioneer; SB = Shade-Bearer.

	Ankasa conservation area		Bia conservation area	
	Producer accuracy %	User accuracy %	Producer accuracy %	User Accuracy %
SB	87.72	89.49	79.35	90.06
NPLD	89.25	91.33	87.26	78.72
PION	96.55	90.08	94.92	86.64
SHADOW	96.31	98.24	93.98	98.85
Overall accuracy	92.34		88.53	
K coefficient	0.92		0.88	

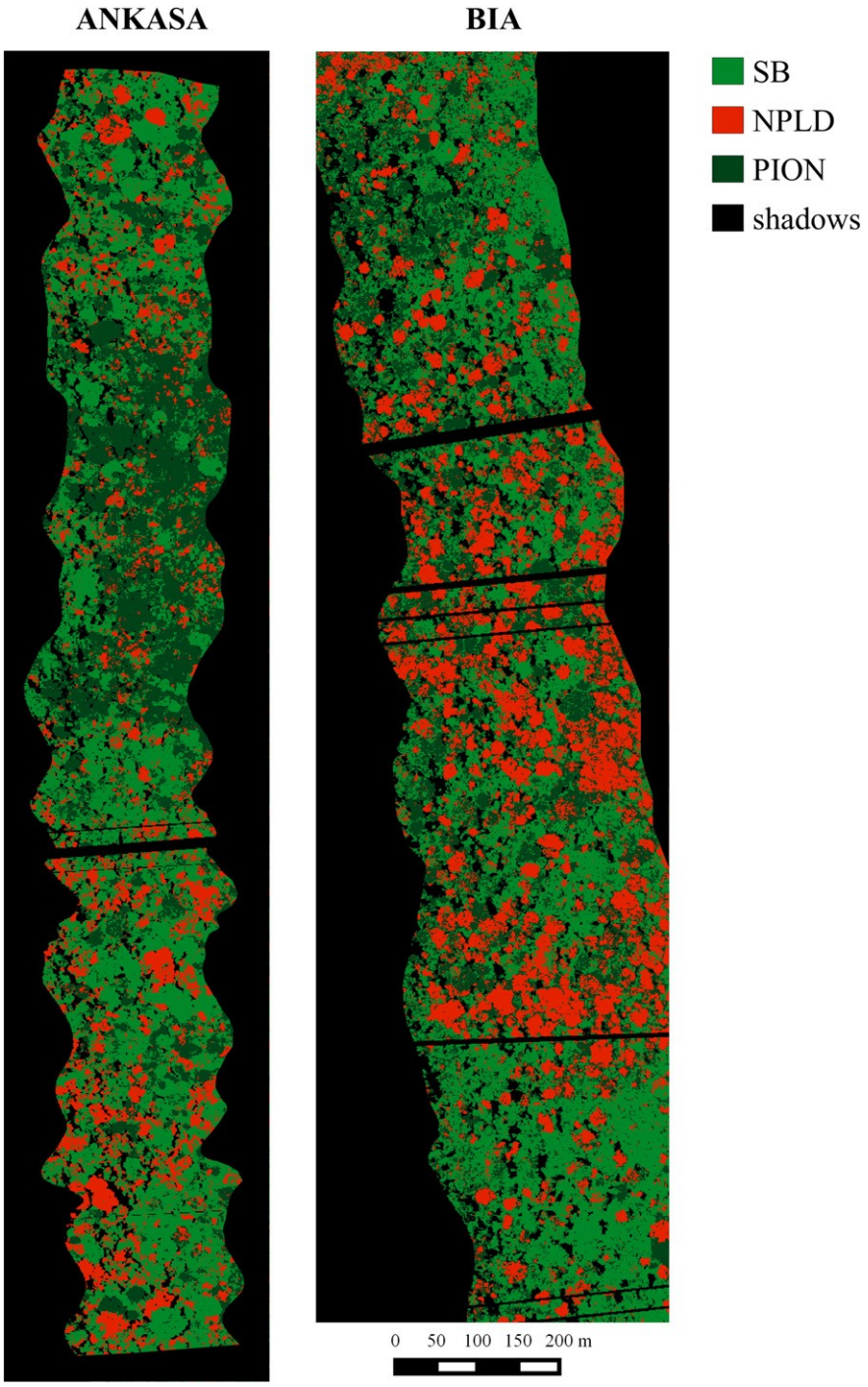

Fig. 5. Guild maps obtained using hypespectral bands and vegetation indices as inputs and Support Vector Machine classification approach.

belonging to the same guild - show marked and different phenological features, such as deciduousness or flowering; these phenological differences in the two NPLD Bia species, observed also in orthophotos, explain the high separability. In this view, the collection of multitemporal acquisitions, planned for the forthcoming Sentinel-2 mission, becomes especially important for species discrimination.

4.3. Functional composition (guilds)

Results from guilds analysis are preliminary and more species from each guild will have to be sampled before any guild-wide signals can be confirmed. If future work confirms or reinforces these differences, quantifying changes of patterns of dominance of different guilds will be possible in tropical forests with hyperspectral data, and there is the potential to perform the same task with forthcoming S2 data (Tables 5 and 6). Patterns of change in guild dominance from wet to dry forest directly indicate response of the plant community to past disturbances; in other words this will provide a metric for stages of secondary growth, with strong potential for improved forest management (Hawthorne, 1996). The better SVM classification results in comparison to the ones from ML, obtained for both areas, highlight the importance of machine learning approaches for performing complex analyses.

The availability of sensors capable of identifying guild is relevant in ecology, especially in regions which are under increasing anthropogenic

and climate change pressure such as West Africa, with forests at risk of functional change and shifts in species ranges. Mapping efforts conducted at species level might be not feasible in tropical forests, where hundreds of species occur: guild dominance mapping may offer a convenient alternative for monitoring forest functional changes, even in areas where plant taxonomy is incomplete or hard to pursue. Presently, the detection of functional changes by means of hyperspectral data is practically unfeasible due to high airborne data collection costs, which limits the area coverage, and the need of specialized expertise for processing and interpretation. However, technological innovation already allowed the development of hyperspectral sensors suited to be accommodated in drones (Suomalainen et al., 2014), and examples of community forest local monitoring by drones at reduced cost are already in place and could be replicated (Paneque-Gálvez, McCall, Napoletano, Wich, & Koh, 2014). Thus, in a near future, these technologies could be employed to support hyperspectral based monitoring in specific sites of high ecological value or critically threatened, as well as to calibrate satellite-based data used in larger scale monitoring efforts.

We separately carried out the guild classification in Ankasa and Bia because the two hyperspectral strips covering these areas were collected under different atmospheric and aerial survey conditions. Additional tests are thus needed to better assess the applicability of the method over larger extents. It is expected that using a satellite sensor such as the S2, which collects data over broad regions, will solve the problems arising when an aerial survey, necessarily fragmented into different flights, is conducted.

The separability results obtained in guild level tests using S2 data are preliminary but encouraging (Table 4), allowing some optimism for future portability of the procedure proposed here, especially considering that additional information will be provided by the full band set. It could be advisable to provide to end users, together with imagery, preprocessed derived features that can increase data utility (i.e. textures and vegetation indices), eliminating these processing steps, and allowing a wider range of users, especially in developing countries in tropical regions, to benefit from the new EO opportunity. However, S2 will generate big data streams requiring large storage facilities and expert knowledge, a fact that has to be properly considered when planning S2 data use.

Furthermore, a guild mapping approach can effectively support large-scale forest inventories, which were the basis in the last decades for providing the information necessary to fulfill reporting obligations under international agreements such as the FAO Global Forest Resource Assessment, the Kyoto protocol, the United Nations Convention on Biological Diversity (Corona, Chirici, McRoberts, Winter, & Barbati, 2011).

Traditionally, the principal aim of national forest inventories is supplying information on forest timber availability and productivity. Despite this, in recent years, more and more attention has been given to forest biodiversity, as is shown, for example, by the consideration of deadwood among principal inventory attributes (Rondeux et al., 2012).

Linking inventory data to ecologically meaningful forest categories like functional guilds brings substantial advantages for forest assessment, since: (i) it allows improved understanding, interpretation and communication of data on biodiversity variables by enabling comparison of ecologically similar forests; (ii) it enables a more detailed and richer analysis of indicators in a specific forest habitat (e.g. the relationship between the vertical structure of forest habitat and vertebrate and invertebrate fauna diversity); and (iii) it provides a suitable basis for estimation by ensuring that different forest habitats are adequately represented in the inventory field plots. Under such operational perspectives, the portability of the main results by the present study (i.e. those concerning guild mapping) is proved by both the general representativeness of selected test areas, the input data availability and the feasibility of the proposed elaboration procedures. Such results emphasize a significant potential of the Sentinel-2 images for improving large-scale forest monitoring and assessment efforts in tropical and subtropical countries, like e.g. those under the mechanisms by UN-REED (2013).

Guild dominance mapping should improve the precision of the inventory estimates, either supporting the initial stratification of the inventory field sample (Corona, 2010) or by coupling the mapped data (used as auxiliary information) with the field sample data (e.g. biomass, merchantable timber) by model-assisted (Corona et al., 2014) or model-based (Meng, Cieszewski, & Madden, 2009) inferential procedures.

In conclusion, this study contributed to an understanding of how forest and ecological research is likely to be helped by advanced remote sensing instruments, and proposed the guild mapping approach as a tool to help efficiently monitor the varied tropical forest resources and their changes. This approach could be of special use in the near future, with the availability of S2 multitemporal data over broad regions, and could support a better understanding of the response of forests to a changing climate.

Hyperspectral high resolution data are possibly the best tool to conduct forest change studies, especially if coupled with sensors able to provide information on vertical forest structure, such as LiDAR. Several satellite hyperspectral missions, with open access policy for scientific use, are under preparation: the EnMAP (Environmental Mapping and Analysis Program) by the Space Agency of the German Aerospace Centre, the HyspIRI mission of the National Aeronautics and Space Administration of the United States, the continuity of PRISMA (Hyperspectral Precursor of the Application Mission) led by the Italian Space Agency, and the HISUI HIS sensor for launch on ALOS-3 satellite by the Japanese Space Agency. Furthermore, micro- and mini-satellites will certainly have a role in future hyperspectral EO missions (Guelman & Ortenberg, 2009). Thus, it is clear that in the coming decade our way to observe and study forests might be radically changed by the availability of these new data. However, in the meanwhile ESA Sentinel-2 will certainly produce very detailed forest information, with additional opportunities coming from its joint use with the already available Sentinel-1 microwave data, paving the road for the development of new concepts and methods in forest monitoring and ecological research.

Acknowledgments

We acknowledge the ERC grant Africa GHG #247349 for providing funding for this research. G.V.L. and D.P. thank the EU for supporting the BACI project funded by the EU's Horizon 2020 Research and Innovation Programme under grant agreement 640176. Our great thanks goes to the personnel of Ghana Forestry Commission and parks staff for helping during the field and aerial surveys, and to Justice Mensah for its valuable field support.

References

Agyeman, V. K., Swaine, M. D., & Thompson, J. (1999). Responses of tropical forest tree seedlings to irradiance and the derivation of a light response index. Journal of Ecology, 87(5), 815–827.

Alvarez-Añorve, M., Quesada, M., & De la Barrera, E. (2008). Remote sensing and plant functional groups detection: physiology, ecology and spectroscopy in tropical systems. Hyperspectral Remote Sensing of Tropical and Sub-Tropical Forests (pp. 27–45). London: Taylor and Francis Group.

Asner G., P., R.E, Martin, Ford, A. J., Metcalfe, D. J., & Liddell, M. J. (2009). Leaf chemical and spectral diversity in Australian tropical forests. Ecological Applications, 19, 236–253.

Asner, G. P., & Vitousek, P. M. (2005). Remote analysis of biological invasion and biogeochemical change. Proceedings of the National Academy of Sciences of the United States of America, 102(12), 4383–4386.

Asner, G. P., Knapp, D. E., Kennedy-Bowdoin, T., Jones, M. O., Martin, R. E., Boardman, J., & Hughes, R. F. (2008). Invasive species detection in Hawaiian rainforests using airborne imaging spectroscopy and LiDAR. Remote Sensing of Environment, 112(5), 1942–1955.

Asner, G. P., Martin, R. E., Knapp, D. E., Tupayachi, R., Anderson, C., Carranza, L., ... Weiss, P. (2011). Spectroscopy of canopy chemicals in humid tropical forests. Remote Sensing of Environment, 115(12), 3587–3598.

Baillarin, S. J., Meygret, A., Dechoz, C., Petrucci, B., Lacherade, S., Tremas, T., ... Spoto, F. (2012, July). Sentinel-2 level 1 products and image processing performances.

Geoscience and Remote Sensing Symposium (IGARSS), 2012. IEEE International. (pp. 7003-7006) IEEE.

Baker, T. R., Swaine, M. D., & Burslem, D. F. (2003). Variation in tropical forest growth rates: combined effects of functional group composition and resource availability. Perspectives Plants Ecology Evolution.and systematics, 6(1), 21-36.

Baldeck, C. A., Colgan, M. S., Féret, J. B., Levick, S. R., Martin, R. E., & Asner, G. P. (2014). Landscape-scale variation in plant community composition of an African savanna from airborne species mapping. Ecological Applications, 24(1), 84-93.

Barbati, A., Corona, P., & Marchetti, M. (2007). A forest typology for monitoring sustainable forest ecosystem management: the case of European Forest Types. Plant Biosystems, 1, 93-103.

Bongers, F., Poorter, L., Hawthorne, W. D., & Sheil, D. (2009). The intermediate disturbance hypothesis applies to tropical forests, but disturbance contributes little to tree diversity. Ecology Letters, 12(8), 798-805.

Burges, C. J. C. (1998). A tutorial on support vector machines for pattern recognition. Data Mining and Knowledge Discovery, 2(2), 121-167 1998.

Canadell, J. G., Pataki, D. E., & Pitelka, L. F. (2007). Terrestrial ecosystems in a changing world. Springer Science & Business Media.

Carlson, K. M., Asner, G. P., Hughes, R. F., Ostertag, R., & Martin, R. E. (2007). Hyperspectral remote sensing of canopy biodiversity in Hawaiian lowland rainforests. Ecosystems, 10(4), 536-549.

Castro-Esau, K. L., Sánchez-Azofeifa, G. A., & Caelli, T. (2004). Discrimination of lianas and trees with leaf-level hyperspectral data. Remote Sensing of Environment, 90(3), 353-372.

Chambers, J. Q., Negron-Juarez, R. I., Marra, D. M., Di Vittorio, A., Tews, J., Roberts, D., ... Higuchi, N. (2013). The steady-state mosaic of disturbance and succession across an old-growth Central Amazon forest landscape. Proceedings of the National Academy of Sciences, 110(10), 3949-3954.

Chan, J. C. W., & Paelinckx, D. (2008). Evaluation of Random Forest and Adaboost tree-based ensemble classification and spectral band selection for ecotope mapping using airborne hyperspectral imagery. Remote Sensing of Environment, 112, 2999-3011.

Chen, Q., Vaglio Laurin, G., & Valentini, R. (2015). Uncertainty of remotely sensed aboveground biomass over an African tropical forest: propagating errors from trees to plots to pixels. Remote Sensing of Environment, 160, 134-143.

Christensen, J. H., Hewitson, B., Busuioc, A., et al. (2007). Regional climate projections. Climate Change, 2007: The physical science basis. Contribution of Working group I to the Fourth Assessment Report of the Intergovernmental Panel on Climate Change (pp. 847-940). Cambridge: University Press Chapter 11.

Clark, D. A., & Clark, D. B. (1999). Assessing the growth of tropical rain forest trees: issues for forest modeling and management. Ecological Applications, 9(3), 981-997.

Clark, M. L., & Roberts, D. A. (2012). Species-level differences in hyperspectral metrics among tropical rainforest trees as determined by a tree-based classifier. Remote Sensing, 4(6), 1820-1855.

Clark, M. L., Roberts, D. A., & Clark, D. B. (2005). Hyperspectral discrimination of tropical rain forest tree species at leaf to crown scales. Remote Sensing of Environment, 96(3), 375-398.

Clark, M. L., Roberts, D. A., Ewel, J. J., & Clark, D. B. (2011). Estimation of tropical rain forest aboveground biomass with small-footprint lidar and hyperspectral sensors. Remote Sensing of Environment, 115(11), 2931-2942.

Condit, R., S.P, Hubbel, & R.B, Foster (1996). Assessing the response of plant functional types to climatic change in tropical forests. Journal of Vegetation Science, 7, 405-476.

Congalton, R. G., & Green, K. (2008). Assessing the accuracy of remotely sensed data: principles and practices. CRC press.

Corona, P. (2010). Integration of forest mapping and inventory to support forest ecosystem management. iForest - Biogeosciences. and Forestry, 3, 59-64.

Corona, P., Chirici, G., McRoberts, R. E., Winter, S., & Barbati, A. (2011). Contribution of large-scale forest inventories to biodiversity assessment and monitoring. Forest Ecology and Management, 262, 2061-2069.

Corona, P., Fattorini, L., Franceschi, S., Chirici, G., Maselli, F., & Secondi, L. (2014). Mapping by spatial predictors exploiting remotely sensed and ground data: a comparative design-based perspective. Remote Sensing of Environment, 152, 29-37.

Culbert, P. D., Radeloff, V. C., St-Louis, V., Flather, C. H., Rittenhouse, C. D., Albright, T. P., & Pidgeon, A. M. (2012). Modeling broad-scale patterns of avian species richness across the Midwestern United States with measures of satellite image texture. Remote Sensing of Environment, 118, 140-150.

Cutler, M. E. J., Boyd, D. S., Foody, G. M., & Vetrivel, A. (2012). Estimating tropical forest biomass with a combination of SAR image texture and Landsat TM data: An assessment of predictions between regions. ISPRS Journal of Photogrammetry and Remote Sensing, 70, 66-77.

D'Odorico, P., Gonsamo, A., Damm, A., & Schaepman, M. E. (2013). Experimental evaluation of Sentinel-2 spectral response functions for NDVI time-series continuity. IEEE Transactions on Geoscience and Remote Sensing, 51(3), 1336-1348.

Dubayah, R. O., Sheldon, S. L., Clark, D. B., Hofton, M. A., Blair, J. B., Hurtt, G. C., & Chazdon, R. L. (2010). Estimation of tropical forest height and biomass dynamics using lidar remote sensing at La Selva, Costa Rica. Journal of Geophysical Research: Biogeosciences, 115(G2) 2005-2012.

Fauset, S., Baker, T. R., Lewis, S. L., et al. (2012). Drought-induced shifts in the floristic and functional composition of tropical forests in Ghana. Ecology Letters, 15, 1120-1129.

Felde, G. W., Anderson, G. P., Cooley, T. W., Matthew, M. W., Adler-Golden, S. M., et al. (2003). Analysis of Hyperion data with the FLAASH Atmospheric Correction Algorithm. Geoscience and Remote Sensing Symposium 2003 IGARSS'03. Proceedings 2003 IEEE International, 1. (pp. 90-92).

Féret, J. B., & Asner, G. P. (2012). Semi-supervised methods to identify individual crowns of lowland tropical canopy species using imaging spectroscopy and LiDAR. Remote Sensing, 4(8), 2457-2476.

Féret, J. B., & Asner, G. P. (2014). Mapping tropical forest canopy diversity using high-fidelity imaging spectroscopy. Ecological Applications, 24(6), 1289-1296.

Foody, G. M. (2003b). Remote sensing of tropical forest environments: Towards the monitoring of environmental resources for sustainable development. International Journal of Remote Sensing, 24(20), 4035-4046.

Foody, G. M., Boyd, D. S., & Cutler, M. E. (2003a). Predictive relations of tropical forest biomass from Landsat TM data and their transferability between regions. Remote Sensing of Environment, 85(4), 463-474.

Foody, G. M., Palubinskas, G., Lucas, R. M., Curran, P. J., & Honzak, M. (1996). Identifying terrestrial carbon sinks: Classification of successional stages in regenerating tropical forest from Landsat TM data. Remote Sensing of Environment, 55(3), 205-216.

Galvão, L. S., Formaggio, A. R., & Tisot, D. A. (2005). Discrimination of sugarcane varieties in Southeastern Brazil with EO-1 Hyperion data. Remote Sensing of Environment, 94(4), 523-534.

Galvão, L. S., Breunig, F. M., Santos, J. R., & Moura, Y. M. (2013). View-illumination effects on hyperspectral vegetation indices in the Amazonian tropical forest. International Journal of Applied Earth Observation and Geoinformation, 21, 291-300.

Gamon, J. A., & Surfus, J. S. (1999). Assessing leaf pigment content and activity with a reflectometer. The New Phytologist, 143, 105-117.

Gamon, J. A., Penuelas, J., & Field, C. B. (1992). A narrow-waveband spectral index that tracks diurnal changes in photosynthetic efficiency. Remote Sensing of Environment, 41, 35-44.

Gibbs, H. K., Brown, S., Niles, J. O., & Foley, J. A. (2007). Monitoring and estimating tropical forest carbon stocks: Making REDD a reality. Environmental Research Letters, 2(4), 045023.

Gitelson, A. A., Merzlyak, M. N., & Chivkunova, O. B. (2001). Optical properties and nondestructive estimation of anthocyanin content in plant leaves. Photochemistry and Photobiology, 71, 38-45.

Gitelson, A. A., Zur, Y., Chivkunova, O. B., & Merzlyak, M. N. (2002). Assessing carotenoid content in plant leaves with reflectance spectroscopy. Photochemistry and Photobiology, 75, 272-281.

Green, A. A., Berman, M., Switzer, P., & Craig, M. D. (1988). A transformation for ordering multispectradata in terms of image quality with implications for noise removal. IEEE Transactions on Geoscience and Remote Sensing, 26, 65-74.

Guelman, M., & Ortenberg, F. (2009). Small satellite's role in future hyperspectral earth observation missions. Acta Astronautica, 64(11), 1252-1263.

Hall, J. B., & Swaine, M. D. (1981). Distribution and ecology of vascular plants in a tropical rain forest: forest vegetation in Ghana. Hague.

Hansen, M. C., Roy, D. P., Lindquist, E., Adusei, B., Justice, C. O., & Altstatt, A. (2008b). A method for integrating MODIS and Landsat data for systematic monitoring of forest cover and change in the Congo Basin. Remote Sensing of Environment, 112(5), 2495-2513.

Hansen, M. C., Stehman, S. V., Potapov, P. V., Loveland, T. R., Townshend, J. R., DeFries, R. S., ... DiMiceli, C. (2008a). Humid tropical forest clearing from 2000 to 2005 quantified by using multitemporal and multiresolution remotely sensed data. Proceedings of the National Academy of Sciences, 105(27), 9439-9444.

Haralick, R. M. (1979). Statistical and structural approaches to texture. Proceedings of the IEEE, 67(5), 786-804.

Hasmadi, I. M., Kamaruzaman, J., & Hidayah, M. N. (2010). Analysis of crown spectral characteristic and tree species mapping of tropical forest using hyperspectral imaging. Journal of Tropical Forest Science, 67-73.

Hawthorne, W., & Abu-Juam, M. (1995). Forest protection in Ghana: with particular reference to vegetation and plant species. Vol. 15, IUCN.

Hawthorne, W., & Gyakari, N. (2006). Photoguide for the forest trees of Ghana: a tree-spotter's field guide for identifying the largest trees. Oxford Forestry Institute, Department of Plant Sciences.

Hawthorne, W. D. (1989, March). The flora and vegetation of Ghana's forests. Ghana forest inventory proceedings (pp. 8-13).

Hawthorne, W. D. (1995). Ecological profiles of Ghanaian forest trees. ODA tropical forestry papers 29. Oxford Forestry Institute 345 pp.

Hawthorne, W. D. (1996). Holes and the sums of parts in Ghanaian forest: Regeneration, scale and sustainable use. Proceedings of the Royal Society of Edinburgh. Section B. Biological Sciences, 104, 75-176.

Hawthorne, W. D., Sheil, D., Agyeman, V. K., Juam, M. A., & Marshall, C. A. M. (2012). Logging scars in Ghanaian high forest: Towards improved models for sustainable production. Forest Ecology and Management, 271, 27-36.

Held, A., Ticehurst, C., Lymburner, L., & Williams, N. (2003). High resolution mapping of tropical mangrove ecosystems using hyperspectral and radar remote sensing. International Journal of Remote Sensing, 24(13), 2739-2759.

Hill, J. L., & Curran, P. J. (2005). Fragment shape and tree species composition in tropical forests: A landscape level investigation. African Journal of Ecology, 43(1), 35-43.

Hill, M. J. (2013). Vegetation index suites as indicators of vegetation state in grassland and savanna: An analysis with simulated SENTINEL 2 data for a North American transect. Remote Sensing of Environment, 137, 94-111.

Kalacska, M., & Sanchez-Azofeifa, G. A. (2008). Hyperspectral remote sensing of tropical and sub-tropical forests. CRC Press.

Kalacska, M., Bohlman, S., Sanchez-Azofeifa, G. A., Castro-Esau, K., & Caelli, T. (2007a). Hyperspectral discrimination of tropical dry forest lianas and trees: Comparative data reduction approaches at the leaf and canopy levels. Remote Sensing of Environment, 109(4), 406-415.

Kalacska, M., Sanchez-Azofeifa, G. A., Rivard, B., et al. (2007b). Ecological fingerprinting of ecosystem succession: Estimating secondary tropical dry forest structure and diversity using imaging spectroscopy. Remote Sensing of Environment, 108, 82.

Karfakis, T. N. S., & Andrade, A. (2013). Dynamics of functional composition of a brazilian tropical forest in response to drought stress. International Journal of Environmental, Ecological, Geological and Geophysical Engineering, 7(3) 2013.

Kaufman, Y. J., & Tanré, D. (1996). Strategy for direct and indirect methods for correcting the aerosol effect on remote sensing: from AVHRR to EOS-MODIS. Remote Sensing of Environment, 55(1), 65–79.

Kokaly, R. F., Asner, G. P., Ollinger, S. V., Martin, M. E., & Wessman, C. A. (2009). Characterizing canopy biochemistry from imaging spectroscopy and its application to ecosystem studies. Remote Sensing of Environment, 113, S78–S91.

Kumagai, T. O., & Porporato, A. (2012). Drought-induced mortality of a Bornean tropical rain forest amplified by climate change. Journal of Geophysical Research: Biogeosciences, 117 2005–2012. G2.

Kumar, L., Schmidt, K., Dury, S., & Skidmore, A. (2001). Imaging spectrometry and vegetation science. In F. D. Van der Meer, & S. M. De ong (Eds.), Imaging Spectrometry: Basic Principles and Prospective Applications (pp. 111–155). Kluwer Academic Publishers.

Lavorel, S., & Garnier, E. (2002). Predicting changes in community composition and ecosystem functioning from plant traits: revisiting the Holy Grail. Functional Ecology, 16(5), 545–556.

Lavorel, S., McIntyre, S., Landsberg, J., & Forbes, T. D. A. (1997). Plant functional classifications: from general groups to specific groups based on response to disturbance. Trends in Ecology & Evolution, 12(12), 474–478.

Lee, K. S., Cohen, W. B., Kennedy, R. E., et al. (2004). Hyperspectral versus multispectral data for estimating leaf area index in four different biomes. Remote Sensing of Environment, 91, 508.

Leutner, B. F., Reineking, B., Müller, J., Bachmann, M., Beierkuhnlein, C., Dech, S., & Wegmann, M. (2012). Modelling forest α-diversity and floristic composition—On the added value of LiDAR plus hyperspectral remote sensing. Remote Sensing, 4(9), 2818–2845.

Lewis, S. L., Phillips, O. L., Baker, T. R., Lloyd, J., Malhi, Y., Almeida, S., ... Vinceti, B. (2004). Concerted changes in tropical forest structure and dynamics: Evidence from 50 South American long-term plots. Philosophical Transactions of the Royal Society of London. Series B: Biological Sciences, 359(1443), 421–436.

Li, G., Lu, D., Moran, E., & Hetrick, S. (2011). Land-cover classification in a moist tropical region of Brazil with Landsat Thematic Mapper imagery. International Journal of Remote Sensing, 32(23), 8207–8230.

Lu, D., Batistella, M., Moran, E., & de Miranda, E. E. (2008). A comparative study of Landsat TM and SPOT HRG images for vegetation classification in the Brazilian Amazon. Photogrammetric Engineering & Remote Sensing, 74(3), 311–321.

Lu, D., Li, G., Moran, E., Dutra, L., & Batistella, M. (2014). The roles of textural images in improving land-cover classification in the Brazilian Amazon. International Journal of Remote Sensing, 35(24), 8188–8207.

Marchetti, M., Vizzarri, M., Lasserre, B., Sallustio, L., & Tavone, A. (2014). Natural capital and bioeconomy: Challenges and opportunities for forestry. Annals of Silvicultural Research, 38, 62–73.

Margono, B. A., Turubanova, S., Zhuravleva, I., Potapov, P., Tyukavina, A., Baccini, A., ... Hansen, M. C. (2012). Mapping and monitoring deforestation and forest degradation in Sumatra (Indonesia) using Landsat time series data sets from 1990 to 2010. Environmental Research Letters, 7(3), 034010.

Marshall, C. A., & Hawthorne, W. D. (2012). Regeneration ecology of the useful flora of the Putu Range Rainforest, Liberia. Economic Botany, 66(4), 398–412.

Martin, M. E., Newman, S. D., Aber, J. D., & Congalton, R. G. (1998). Determining forest species composition using high spectral resolution remote sensing data. Remote Sensing of Environment, 65(3), 249–254.

McDowell, N. G., Coops, N. C., Beck, P. S., Chambers, J. Q., Gangodagamage, C., Hicke, J. A., ... Allen, C. D. (2015). Global satellite monitoring of climate-induced vegetation disturbances. Trends in Plant Science, 20(2), 114–123.

Meng, Q. M., Cieszewski, C., & Madden, M. (2009). Large area forest inventory using Landsat ETM plus: A geostatistical approach. ISPRS Journal of Photogrammetry and Remote Sensing, 64(1), 27–36.

Mountrakis, G., Im, J., & Ogole, C. (2011). Support vector machines in remote sensing: A review. ISPRS Journal of Photogrammetry and Remote Sensing, 66(3–66), 247–259.

Mulkey, S. S., Wright, S. J., & Smith, A. P. (1993). Comparative physiology and demography of three Neotropical forest shrubs: Alternative shade-adaptive character syndromes. Oecologia, 96(4), 526–536.

Paneque-Gálvez, J., Mas, J. F., Moré, G., Cristóbal, J., Orta-Martínez, M., Luz, A. C., ... Reyes-García, V. (2013). Enhanced land use/cover classification of heterogeneous tropical landscapes using support vector machines and textural homogeneity. International Journal of Applied Earth Observation and Geoinformation, 23, 372–383.

Paneque-Gálvez, J., McCall, M. K., Napoletano, B. M., Wich, S. A., & Koh, L. P. (2014). Small drones for community-based forest monitoring: An assessment of their feasibility and potential in tropical areas. Forests, 5(6), 1481–1507.

Papes, M., Tupayachi, R., Martinez, P., Peterson, A. T., Asner, G. P., & Powell, G. V. N. (2013). Seasonal variation in spectral signatures of five genera of rainforest trees. IEEE Journal of Selected Topics in Applied Earth Observations and Remote Sensing, 6(2), 339–350.

Phillips, O. L., Van der Heijden, G., Lewis, S. L., López-González, G., Aragão, L. E., Lloyd, J., ... Silveira, M. (2010). Drought–mortality relationships for tropical forests. New Phytologist, 187(3), 631–646.

Pirotti, F., Vaglio Laurin, G. V., Vettore, A., Masiero, A., & Valentini, R. (2014). Small footprint full-waveform metrics contribution to the prediction of biomass in tropical forests. Remote Sensing, 6(10), 9576–9599.

R Core Team (2013). R: A language and environment for statistical computing. Vienna, Austria: R Foundation for Statistical Computing URL http://www.R-project.org/.

Rakwatin, P., Longépé, N., Isoguchi, O., Shimada, M., Uryu, Y., & Takeuchi, W. (2012). Using multiscale texture information from ALOS PALSAR to map tropical forest. International Journal of Remote Sensing, 33(24), 7727–7746.

Reich, P. B., Wright, I. J., Cavender-Bares, J., Craine, J. M., Oleksyn, J., Westoby, M., & Walters, M. B. (2003). The evolution of plant functional variation: Traits, spectra, and strategies. International Journal of Plant Sciences, 164(S3), S143–S164.

Richards, J. A., & Jia, X. (1999). Remote Sensing digital imaging analysis: an introduction (3rd ed.). Berlin: Springer.

Richter, K., Atzberger, C., Vuolo, F., Weihs, P., & d'Urso, G. (2009). Experimental assessment of the Sentinel-2 band setting for RTM-based LAI retrieval of sugar beet and maize. Canadian Journal of Remote Sensing, 35(3), 230–247.

Rondeux, J., Bertini, R., Bastrup-Birk, A., Corona, P., Latte, N., McRoberts, R. E., ... Chirici, G. (2012). Assessing deadwood using Harmonized National Forest Inventory Data. Forest Science, 58(3), 269–283.

Saini, M., Christian, B., Joshi, N., Vyas, D., Marpu, P., & Krishnayya, N. S. R. (2014). Hyperspectral Data Dimensionality Reduction and the Impact of Multi-seasonal Hyperion EO-1 Imagery on Classification Accuracies of Tropical Forest Species. Photogrammetric Engineering & Remote Sensing, 80(8), 773–784 0099–1112/14/8007–773.

Sánchez-Azofeifa, G. A., & Castro-Esau, K. (2006). Canopy observations on the hyperspectral properties of a community of tropical dry forest lianas and their host trees. International Journal of Remote Sensing, 27(10), 2101–2109.

Sellers, P. J. (1985). Canopy reflectance, photosynthesis and transpiration. International Journal of Remote Sensing, 6(8), 1335–1372.

Shafri, H. Z. M., Hamdan, N., & Izzuddin Anuar, M. (2012). Detection of stressed oil palms from an airborne sensor using optimized spectral indices. International Journal of Remote Sensing, 33(14), 4293–4311.

Sheffield, J., & Wood, E. F. (2008). Projected changes in drought occurrence under future global warming from multi-model, multi-scenario, IPCC AR4 simulations. Climate Dynamics, 31, 79–105.

Sheil, D., Salim, A., Chave, J., Vanclay, J., & Hawthorne, W. D. (2006). Illumination-size relationships of 109 coexisting tropical forest tree species. Journal of Ecology, 94(2), 494–507.

Simberloff, D., & Dayan, T. (1991). The guild concept and the structure of ecological communities. Annual Review of Ecology and Systematics, 115-143.

Sims, D. A., & Gamon, J. A. (2002). Relationships between leaf pigment content and spectral reflectance across a wide range of species, leaf structures and developmental stages. Remote Sensing of Environment, 81(2), 337–354.

Smith, T. M., Shugart, H. H., & Woodward, F. I. (1997). Plant functional types: their relevance to ecosystem properties and global change. Vol. 1, Cambridge University Press.

Somers, B., & Asner, G. P. (2012). Hyperspectral time series analysis of native and invasive species in Hawaiian rainforests. Remote Sensing, 4(9), 2510–2529.

Somers, B., & Asner, G. P. (2013). Invasive species mapping in Hawaiian rainforests using multi-temporal Hyperion spaceborne imaging spectroscopy. Selected Topics in Applied Earth Observations and Remote Sensing, IEEE Journal of, 6(2), 351–359.

Somers, B., & Asner, G. P. (2014). Tree species mapping in tropical forests using multi-temporal imaging spectroscopy: Wavelength adaptive spectral mixture analysis. International Journal of Applied Earth Observation and Geoinformation, 31, 57–66.

Suomalainen, J., Anders, N., Iqbal, S., Roerink, G., Franke, J., Wenting, P., ... Kooistra, L. (2014). A lightweight hyperspectral mapping system and photogrammetric processing chain for unmanned aerial vehicles. Remote Sensing, 6(11), 11013–11030.

Terborgh, J., & Robinson, S. (1986). Guilds and their utility in ecology. In J. Kikkawa, & D. J. Anderson (Eds.), Community Ecology: Patterns and Processes (pp. 65–90). Oxford, UK: Blackwell Scientific Publications.

Thenkabail, P. S., Lyon, J. G., & Huete, A. (2011). Hyperspectral remote sensing of vegetation. CRC Press.

Thenkabail, P. S., Enclona, E. A., Ashton, M. S., et al. (2004). Hyperion, IKONOS, ALI, and ETM+ sensors in the study of African rainforests. Remote Sensing of Environment, 90, 23.

UN-REDD (2013). National Forest Monitoring Systems: Monitoring and Measurement, Reporting and Verification (M & MRV) in the context of REDD+ Activities. Rome: FAO.

Ustin, S. L., Roberts, D. A., Gamon, J. A., Asner, G. P., & Green, R. O. (2004). Using imaging spectroscopy to study ecosystem processes and properties. Bioscience, 54, 523–534.

Vaglio Laurin, G., Chan, J. C. W., Chen, Q., Lindsell, J. A., Coomes, D. A., Guerriero, L., ... Valentini, R. (2014). Biodiversity mapping in a tropical west african forest with airborne hyperspectral data. PloS One, 9(6), e97910.

Vaglio Laurin, G., Liesenberg, V., Chen, Q., Guerriero, L., Del Frate, F., Bartolini, A., ... Valentini, R. (2013). Optical and SAR sensor synergies for forest and land cover mapping in a tropical site in West Africa. International Journal of Applied Earth Observation and Geoinformation, 21, 7–16.

Verrelst, J., Muñoz, J., Alonso, L., Delegido, J., Rivera, J. P., Camps-Valls, G., & Moreno, J. (2012). Machine learning regression algorithms for biophysical parameter retrieval: Opportunities for Sentinel-2 and-3. Remote Sensing of Environment, 118, 127–139.

Vicharnakorn, P., Shrestha, R. P., Nagai, M., Salam, A. P., & Kiratiprayoon, S. (2014). Carbon Stock Assessment Using Remote Sensing and Forest Inventory Data in Savannakhet, Lao PDR. Remote Sensing, 6(6), 5452–5479.

Viña, A., & Gitelson, A. A. (2011). Sensitivity to foliar anthocyanin content of vegetation indices using green reflectance. Geoscience and Remote Sensing Letters, IEEE, 8(3), 464–468.

Vogelmann, J. E., Rock, B. N., & Moss, D. M. (1993). Red edge spectral measurements from sugar maple leaves. International Journal of Remote Sensing, 14(8), 1563–1575.

Woodward, F. I., & Cramer, W. (1996). Plant functional types and climatic changes: Introduction. Journal of Vegetation Science, 7, 306–308.

Yoneda, T., Nishimura, S., Fujii, S., & MUKHTAR, E. (2009). Tree guild composition of a hill dipterocarp forest in West Sumatra, Indonesia. Tropics, 18(3), 143–154.

Zhang, J., Rivard, B., Sánchez-Azofeifa, A., & Castro-Esau, K. (2006). Intra-and inter-class spectral variability of tropical tree species at La Selva, Costa Rica: Implications for species identification using HYDICE imagery. Remote Sensing of Environment, 105(2), 129–141.

Zhang, Y., Peng, C., Li, W., Fang, X., Zhang, T., Zhu, Q., ... Zhao, P. (2013). Monitoring and estimating drought-induced impacts on forest structure, growth, function, and ecosystem services using remote-sensing data: recent progress and future challenges. Environmental Reviews, 21(2), 103–115.

Zhu, Z., Woodcock, C. E., & Olofsson, P. (2012). Continuous monitoring of forest disturbance using all available Landsat imagery. Remote Sensing of Environment, 122, 75–91.